The Role of Myo2, a Yeast Class V Myosin, in Vesicular Transport

Brinda Govindan, Robert Bowser, and Peter Novick

Department of Cell Biology, Yale University School of Medicine, New Haven, Connecticut 06520-8002

Abstract. Previous studies have shown that temperature-sensitive, *myo2-66* yeast arrest as large, unbudded cells that accumulate vesicles within their cytoplasm (Johnston, G. C., J. A. Prendergast, and R. A. Singer. 1991. *J. Cell Biol.* 113:539–551). In this study we show that *myo2-66* is synthetically lethal in combination with a subset of the late-acting *sec* mutations. Thin section electron miscoscopy shows that the post-Golgi blocked secretory mutants, *sec1-1* and *sec6-4*, rapidly accumulate vesicles in the bud, upon brief incubations at the restrictive temperature. In contrast, *myo2-66* cells accumulate vesicles predominantly in the mother cell. Double mutant analysis also places Myo2 function in a post-Golgi stage of the secretory pathway. Despite the accumulation of vesicles in *myo2-66* cells, pulse-chase studies show that the transit times of several secreted proteins, including invertase and α factor, as well as the vacuolar proteins, carboxypeptidase Y and alkaline phosphatase, are normal. Therefore the vesicles which accumulate in this mutant may function on an exocytic pathway that transports a set of cargo proteins that is distinct from those analyzed. Our observations are consistent with a role for Myo2 in transporting a class of secretory vesicles from the mother cell along actin cables into the bud.

THE yeast *Saccharomyces cerevisiae* exhibits a high degree of cell polarity. The localized incorporation of cell surface constituents causes the daughter cell to approach the size of the mother cell at which time cell division ensues. Bud initiation as well as bud development rely on a wide array of gene products including *ACT1*, *BUD1-5*, *BEM1*, *CDC24*, *CDC42*, and *CDC43* (for a recent review see Madden et al., 1992). Polarized growth occurs via the fusion of secretory vesicles with the plasma membrane of the bud. Recent work (Preuss et al., 1992) suggests that components of the secretory pathway, such as the ER and Golgi complex, may be transported into the bud to enable polarized growth. A polarized actin cytoskeleton is associated with the localized deposition of cell surface components (Adams and Pringle, 1984; Kilmartin and Adams, 1984), whereas intact microtubules are not necessary for this process (Huffaker et al., 1988). Temperature-sensitive mutations in the essential yeast gene encoding actin, *ACT1*, result in vesicle accumulation, the predominance of unbudded cells, and the accumulation of the secretory protein invertase within cells at the restrictive temperature (Novick and Botstein, 1985).

A variety of proteins which interact with actin have been identified in yeast (see references within Welch et al., 1994; Brown, 1993; Bretscher et al., 1994). These include yeast capping protein (Cap1 and Cap2) (Amatruda et al., 1990), actin-binding protein (Abp1), fimbrin (Sac6), profilin (Pfy1), cofilin (Cof1), and tropomyosin (Tpm1). *SLA1* and *SLA2* encode proteins required for the formation of the cortical actin cytoskeleton (Holtzman et al., 1993). Recently, the requirement for actin and fimbrin in yeast endocytosis has been demonstrated (Kubler and Riezman, 1993). The characterization of the yeast actin cytoskeleton at the ultrastructural level has provided new insight into its possible functions in the cell. Cortical actin patches were found associated with the cell surface via plasma membrane invaginations, giving rise to speculations about the role of this structure in cell wall growth (Mulholland et al., 1994). Since polarized growth in yeast is associated with a polarized actin cytoskeleton, it has been suggested that an actin-based motor fulfills the role of transporting vesicles into the bud.

To date, four myosins have been identified in yeast. First, the *MYO1* gene product was identified as the conventional (or class II) myosin in yeast and shown to be required for cytokinesis (Watts et al., 1987). A class I myosin, Myo3, has been identified, but its function is as yet unknown (Goodson, H. V., and J. A. Spudich. 1993. *Mol. Biol. Cell.* 4:156a). In the past few years, a rapidly growing number of unconventional myosins have been identified from a variety of organisms (Cheney and Mooseker, 1992). The yeast *MYO2* and *MYO4* gene products are class V myosins (Johnston et al., 1991; Haarer et al., 1994). They contain a myosin-like head domain which is conserved among the members of this class, a series of IQ motifs involved in calmodulin binding, and a relatively short coiled-coil region followed by a globular distal tail domain. The COOH-terminal portion of these myo-

Address all correspondence to Dr. Peter Novick, Department of Cell Biology, Yale University School of Medicine, 333 Cedar Street, New Haven, CT 06520-8002. Tel.: (203) 785-5871. Fax: (203) 785-7226.

The current address of Dr. Robert Bowser is Division of Neuropathology, University of Pittsburgh, 200 Lothrop Street, PA 15213.

sins are more similar to each other than to any other myosins.

Class V myosins have been implicated in the transport of membrane-bounded organelles in a variety of organisms (Titus, 1993). Mutations in the murine *Dilute* locus, which encodes an essential class V myosin, leads to the loss of coat color in *dilute* mice (Mercer et al., 1991). This phenotype arises from a defect in the transfer of pigment-containing melanosomes into the keratinocytes of the developing hair shaft. Melanosomes in *dilute* mice exhibit mostly a perinuclear distribution, whereas in wild-type mice the melanosomes are evenly distributed between the cell body and dendrites (Wei, M. C., V. Ipe, and J. Mercer. 1994. *Mol. Biol. Cell.* 5:381a). More severe alleles of *dilute* result in death from neurological seizures. An additional member of the class V myosin family is the chick brain myosin V protein (Espindola et al., 1992). Chick brain myosin V has been well-characterized biochemically as an actin-activated ATPase, and it has been localized to the perinuclear region and the tips of cellular processes in neurons (Espreafico et al., 1992; Cheney et al., 1993). This localization suggests an association of chick myosin V with vesicles. Temperature-sensitive *myo2-66* mutants, defective in a yeast class V myosin, arrest as large, unbudded cells with mislocalized actin and chitin (Johnston et al., 1991). Furthermore, *myo2-66* cells accumulate vesicles throughout their cytoplasm upon shifts to the restrictive temperature. Nonetheless, the periplasmic enzyme invertase is still secreted in *myo2-66* mutants. Based on these findings Johnston et al. (1991) proposed that Myo2 functions as a motor to transport post-Golgi secretory vesicles into the growing bud. It was hypothesized that the vesicle accumulation in this mutant is due to a kinetic lag in their transport, since the vesicle motor is defective.

To investigate the possible role of Myo2 in various vesicular transport pathways, we have further characterized the *myo2-66* mutant through analysis of genetic interactions, epistasis tests and through pulse-chase studies of protein transport. Using electron microscopy, we have also examined the phenotype of *myo2-66* cells shifted to 37°C for short time periods to determine the primary site of vesicle accumulation. These studies indicate that Myo2 is involved in a post-Golgi stage of the secretory pathway. Our observations are consistent with the model that Myo2 functions to transport vesicles from the mother cell into the bud.

Materials and Methods

Yeast Strains, Media, and Reagents

The *Saccharomyces cerevisiae* strains used in this study are described in Table I. Cells were grown in YP medium containing 1% Bacto-yeast extract and 2% Bacto-peptone (Difco Laboratories Inc., Detroit, MI), with either 2% glucose (rich medium, YPD) or 0.1% glucose (low glucose media). To change the growth medium, cells were pelleted and resuspended in prewarmed, fresh medium. For the pulse-chase studies, cells were grown in minimal media containing 0.7% yeast nitrogen base without amino acids (Difco), 2% glucose, and supplemented for auxotrophic requirements as described by Sherman et al. (1974) when necessary. The absorbance of cell suspensions was measured at 599 nm in a model No. 4054 spectrophotometer (Pharmacia LKB Biotechnology, Piscataway, NJ).

Sorbitol, α factor, PMSF, Protease Inhibitor Cocktail-PIC (1 mg/ml each of leupeptin, chymostatin, pepstatin, aprotinin, and antiparin), Pronase E, nocodazole, and Triton X-100 were obtained from Sigma Chem. Co. (St. Louis, MO). Chemicals for SDS-PAGE were obtained from BioRad Laboratories (Richmond, CA). SPURR embedding medium for electron microscopy was obtained from Polysciences, Inc. (Worthington, PA). ^{35}S-*trans* label and Zymolyase 100-T were purchased from ICN ImmunoBiologicals (Costa Mesa, CA). [^{35}S] In vitro cell-labeling mix was purchased from Amersham Corp. (Arlington Heights, IL).

Table I. Yeast Strains

Strain	
NY 3	*MATa ura3-52 sec 1-1*
NY 13	*MATa ura3-52*
NY 17	*MATa ura3-52 sec 6-4*
NY 57	*MATa ura3-52 sec 9-4*
NY 61	*MATa ura3-52 sec 10-2*
NY 64	*MATa ura3-52 sec 15-1*
NY 130	*MATa ura3-52 sec 2-41*
NY 180	*MATα ura3-52 leu2-3,112*
NY 402	*MATa ura3-52 sec 5-24*
NY 405	*MATa ura3-52 sec 4-8*
NY 410	*MATa ura3-52 sec 8-9*
NY 412	*MATa ura3-52 sec 3-2*
NY 414	*MATa ura3-52 sec 13-1*
NY 415	*MATa ura3-52 sec 16-2*
NY 418	*MATa ura3-52 sec 17-1*
NY 420	*MATa ura3-52 sec 19-1*
NY 422	*MATa ura3-52 sec 20-1*
NY 426	*MATa ura3-52 sec 22-3*
NY 430	*MATa ura3-52 sec 14-3*
NY 431	*MATa ura3-52 sec 18-1*
NY 579	*MATα pep4::URA3 leu2-3,112*
NY 738	*MATa ura3-52 sec 12-4*
NY 756	*MATa ura3-52 sec 7-1*
NY 829*	*MATa his6 ura1 myo2-66*
NY 830*	*MATα his6 ura1 myo2-66*
NY 895‡	NY 830 × NY 17
NY 896‡	NY 830 × NY 431
NY 919‡	NY 830 × NY 756
NY 922‡	NY 830 × NY 414
NY 1005‡	*MATα ura3-52 leu2-3,112 myo2-66*
NY 1006‡	*MATa ura3-52 leu2-3,112 myo2-66*
NY 1031‡	NY 1006 transformed to Ura+ with pRB58 (*SUC2* on 2 μm plasmid)
NY 1032‡	NY 1033 transformed to Ura+ with pRB58
NY 1033‡	*MATa ura3-52 leu2-3,112*
NY 1125‡	*MATα myo2-66 his4-619 pep4::URA3*
NY 1180§	*MAT a end4::LEU2 bar1-1 lys2 ura3-52 his4-619 leu2-3,112*
NY 1235‡	*MAT α myo2-66 end4::LEU2 ura3-52*

* from G. Johnston.
‡ This study.
§ from H. Riezman.

Yeast Genetic Techniques

Yeast transformation was performed by the alkali cation treatment method (Ito et al., 1983) and transformants were selected on minimal medium supplemented by the appropriate amino acids at 25°C. Crosses of strains, sporulation of diploids, tetrad dissections, complementation, and mating type determination were performed as described by Sherman et al. (1974). Double mutants were constructed between *myo2-66* and various *sec* or *end* genes by crossing the appropriate strains, sporulating the diploids at 25°C, and dissecting the resulting tetrads. In cases where 2:2 segregation of temperature sensitive: temperature-resistant spores was observed, the temperature-sensitive spores were picked and tested for mating type and auxotrophy. *MATa* spores were selected and complementation analysis confirmed that the strains were defective in both *MYO2* and *SEC* or *END* genes.

Thin Section Electron Microscopy

Cells were grown overnight in YPD medium to an A_{599} of 1.0. For synchronization experiments, 13.2 OD units were harvested and incubated in

60 ml of YPD, pH 4.0, containing 1 μM α factor for 4.5 h at 25°C. Cells were then washed in YP, resuspended in 60 ml fresh YPD, and incubated at 25°C for 1 h to induce small bud formation. Temperature shifts were then performed by incubating the cells at 37°C for short periods. At time points, cells were harvested by filtration and washed with 10 ml 0.1 M cacodylate, pH 6.8, reharvested and resuspended in 10 ml cacodylate, pH 6.8, containing 3% glutaraldehyde. After 1 h at room temperature, the cells were incubated on ice overnight at 4°C. Fixed cells were then washed twice in 50 mM phosphate buffer, pH 7.0, and incubated in 2 ml 50 mM phosphate buffer, pH 7.0, containing 0.125 mg/ml Zymolyase 100-T for 40 min at 37°C. After being washed twice in ice cold 0.1 M cacodylate buffer, the cells were resuspended in 2 ml 0.1 M cacodylate with 2% OsO_4 and incubated for 1 h at 4°C. The cells were washed in sterile H_2O three times, resuspended in 2 ml of 2% aqueous uranyl acetate, and incubated at room temperature for 1 h. This was followed by two washes in sterile H_2O, formation into 2% agar blocks, and finally dehydration by a series of graded ethanol washes (1 wash each of 50, 70, 90, and 100% EtOH, and then four washes of fresh 100% EtOH). The dehydrated blocks were washed in 100% acetone and embedded in SPURR epoxy medium. Thin sections were cut, stained with lead citrate, and poststained with uranyl acetate. Sections were analyzed on a Philips 301 electron microscope at 80 kV.

To count vesicles, budded cells containing a nucleus and/or vacuole and a well-defined neck region were selected at random at low magnification. The neck region was considered as part of the mother cell in determining vesicle density in the mother vs the bud. Only vesicles whose membranes could be clearly distinguished were counted. The cytoplasmic area of each cell was determined on a Zeiss MOP-3 magnetized tablet (Carl Zeiss, Inc.) by outlining the surface of each mother cell and bud, and subtracting all internal surfaces including the nucleus, mitochondria, lipid droplets, and vacuoles. The number of vesicles per μm^2 was determined for both the mother and bud of each cell. At least 25–30 samples from 1–3 independent experiments were analyzed per time point.

Pulse Chase Experiments

myo2-66 and wild-type (NY 1006 and NY 1033) strains were transformed to Ura+ with pRB58, a high copy number (2 μm) plasmid containing the *SUC2* gene which encodes invertase (Carlson and Botstein, 1982). The resulting invertase-overproducing strains were grown overnight in supplemented minimal media with 2% glucose at 25°C to an OD_{599} of 0.5. 25 OD units of cells were harvested by centrifugation and resuspended in medium containing 0.1% glucose to derepress invertase synthesis. After incubation in this medium for 30 min at 25°C, cells were pelleted and resuspended in 25 ml of spheroplast buffer containing 0.1% glucose, 1 M sorbitol, 50 mM KPi (pH 7.5), 50 mM β-mercaptoethanol, and 1 mg of Zymolyase-100 T. Spheroplasts were formed by incubation at 25°C for 90 min with gentle agitation, and then pelleted gently and resuspended in 50 ml recovery buffer containing supplemented minimal media, 0.1% glucose, 1 M sorbitol, and 20 mM Pipes (pH 6.6). The spheroplasts were incubated at 25°C for 60 min to allow cell metabolism to return to normal levels. The recovered spheroplasts were then shifted to 37°C for 30 min, pelleted gently and resuspended in 1 ml of recovery buffer. After incubating the recovered spheroplasts for 10 min at 37°C, ^{35}S-*trans* label was added to 0.3 mCi/ml and the spheroplasts were labeled for 4 min at 37°C. The chase was initiated by the addition of cysteine and methionine (in recovery buffer) to a final concentration of 5 mM. At various time points of chase (at 37°C), cell aliquots were removed to tubes on ice and pelleted in a microfuge to separate cells from supernatants (containing the periplasm). The cell pellets were resuspended in 100 μl of 1% SDS and the supernatants were made 1% in SDS and both samples were boiled for 3 min. Both samples were diluted with 900 μl of IP buffer (2% Triton X-100 in PBS) and microcentrifuged for 10 min at 4°C to remove insoluble material. The supernatants were added to tubes containing 2 μl anti-invertase antibody (generous gift of Dr. Susan Ferro-Novick) and incubated overnight at 4°C. The immunoprecipitates were collected on protein A–Sepharose beads (60 μl of a 3% suspension per sample), washed twice with urea wash buffer containing 2 M urea-200 mM NaCl- 100 mM Tris (pH 7.2)- 1% Triton X-100, washed twice with 0.5% β-mercaptoethanol and solubilized by boiling in 50 μl 1× SDS sample buffer for 5 min. Aliquots were counted by liquid scintillation, and 30-μl samples were loaded onto 10% SDS polyacrylamide gels with prestained high molecular weight markers (BRL). The gels were fixed in 0.5 M sodium salicylate-20% MeOH-1% glycerol, dried, and exposed to Kodak X-OMAT film overnight at −70°C.

The secretion of glycoproteins was also examined by a similar method. Cells were spheroplasted as above, and then regenerated in recovery buffer containing 2% glucose for 1 h at 25°C. Nocodazole (15 μg/ml plus 1% DMSO) or just DMSO alone was added to the recovering spheroplasts for 30 min at 37°C. After centrifuging at 2,000 rpm for 5 min, the regenerated spheroplasts were resuspended in 1 ml of recovery buffer. At this point, aliquots were removed, fixed, and processed for immunofluorescence microscopy with anti-tubulin antibody to determine the effectiveness of nocodazole treatment. The regenerated spheroplasts were incubated at 37°C for 10 min, ^{35}S-*trans* label was added to 0.3 mCi/ml for 5 min at 37°C, chase buffer was added (50 mM cysteine/methionine), and at time points aliquots were removed and microcentrifuged to separate the cellular and external (secreted) fraction. In these experiments, the cellular fraction was discarded, while the supernatant (containing secreted proteins) was boiled in 1% SDS. Samples were diluted by the addition of 1 ml of HSW containing 1% TX-100, 0.5 M NaCl, 20 mM Tris-Cl, pH 7.5, and clarified in a microfuge for 15 min. The samples were precipitated with 100 μl of a 20% slurry of Con A Sepharose for 2 h at 4°C. The Con A precipitates were washed with the following: (1% TX-100, 0.1% SDS, 0.15 M NaCl, 15 mM Tris, pH 7.5), (2 M urea, 1% TX-100, 0.2 M NaCl, 0.1 M Tris, pH 7.5), HSW, and LSW (10 mM Tris, pH 7.5, 50 mM NaCl). The samples were then boiled in SDS sample buffer and 30 μl loaded onto 10% SDS polyacrylamide gels and processed for autoradiography as described.

To examine the transit times of carboxypeptidase Y (CPY)[1] and alkaline phosphatase (ALP), a modification of the above protocol was used. 1 OD unit per sample per time point was incubated at 37°C for 30 min. The cells were pelleted and resuspended in 0.5 ml of prewarmed media, and then 100 μCi of ^{35}S-*trans* label was added for 2 min (for CPY) or 5 min (for ALP) at 37°C. Cells were chased with medium containing 10 mM cysteine and methionine, and at time points cell aliquots were removed and washed twice in 1 ml of 10 mM NaN_3. The cell pellets were frozen in liquid nitrogen and thawed on ice to aid lysis. Cells were lysed by vortexing for 3 min at 4°C in the presence of 100 μl 1% SDS and glass beads. The lysates were boiled immediately for 3 min, diluted with 0.9 ml of IP buffer and clarified by pelleting in a microfuge for 15 min at 4°C. The supernatants were added to tubes containing either anti-CPY antibody or anti-alkaline phosphatase antibody (generous gift of Dr. Tom Stevens) and incubated overnight at 4°C. Immunoprecipitates were collected as described above and washed three times in urea wash buffer, and then twice in 1% β-mercaptoethanol. Samples were boiled in SDS sample buffer containing βme for 5 min, and then loaded onto either 8 or 10% SDS gels and treated as described above.

Pulse chase experiments to study the life cycle of the a-factor receptor were also done by labeling intact cells as described in Davis et al. (1993). For protease susceptibility experiments, *PEP4* deficient cells were used. 0.15 OD units of cells per sample per time point were shifted to 30°C for 30 min and labeled with 0.15 mCi ^{35}S in vitro labeling mix for 10 min. Cells were chased with 10 mM cysteine and methionine in media at 30°C. At time points, cell aliquots were removed, made 10 mM in both NaN_3 and KF and kept on ice. All samples were washed once in 10 mM KF and NaN_3, and then resuspended in 100 μl digestion buffer (DB) containing 1.4 M sorbitol, 10 mM KF, 10 mM NaN_3, and 25 mM Tris-Cl, pH 7.5, plus 0.5% β-mercaptoethanol for 30 min at 37°C before being digested with 1 mg/ml Pronase E at 37°C for 1 h. Protease was washed away by two washes in DB containing 1 mM PMSF, and then the samples were treated with DB plus 0.05 mg/ml Zymolyase 100-T and 0.3% β-mercaptoethanol for 30 min at 30°C. The spheroplasts were gently pelleted then resuspended in 50 μl of lysis buffer containing 8 M urea, 2.5% SDS, 40 mM Tris, pH 6.8, 0.1 mM EDTA and 1% β-mercaptoethanol. These samples were boiled for 5 min, diluted with 0.9 ml of IP buffer containing 10 mM Tris-Cl, pH 8.0, 0.1% Triton-X-100, 2 mM EDTA, 1 mM PMSF, and 1:1,000 vol of PIC and clarified as described above. The supernatant was removed to a tube containing 3 μl of anti-STE3 antibody (generous gift of Dr. George Sprague) plus 70 μl of a 3% suspension of protein A–Sepharose CL4B and incubated for 90 min at 4°C. (The antibody was first preadsorbed to the protein A–Sepharose beads for 4 h at 4°C). An aliquot of the supernatant was also counted by liquid scintillation. Immunoprecipitates were collected as described above and washed four times with IP buffer plus 0.1% SDS. The samples were then boiled for 5 min in SDS sample buffer with β-mercaptoethanol, counted by liquid scintillation and loaded on 10% SDS gels with prestained high molecular weight standards. After electrophoresis, the gels were treated as described above.

Secretion of α factor was examined by the method described in Graham and Emr (1991). MATα cells were grown to mid-log phase in supplemented minimal media with 2% glucose overnight at 25°C, and then 10 0DU/ml cells in media containing 1 mg/ml BSA were shifted to 37°C for 30 min.

1. *Abbreviations used in this paper*: ALP, alkaline phosphatase; CPY, carboxypeptidase Y; DB, digestion buffer; wt, wild type.

Whole cells were pulse labeled at 37°C for 8 min with 200 μCi/ml ^{35}S-*trans* label (or in vitro labeling mix), and then chased with 10 mM cysteine and methionine in media. At time points, cell aliquots were removed and pelleted in a microfuge to separate cells from media. Both samples were precipitated with 5% TCA to terminate the chase, washed twice in cold acetone, dried, resuspended in 100 μl buffer containing 50 mM Tris, pH 7.5, 6 M urea, 1 mM EDTA, 1% SDS, and lysed by vortexing with glass beads. After boiling the samples, a MATa lysate of equivalent cell density was added to reduce background in the immunoprecipitation. 900 μl of dilution buffer containing 1.25% TX-100, 190 mM NaCl, 6 mM EDTA, and 50 mM Tris, pH 7.5, was added to each sample. Samples were clarified as described above, and then anti-α factor antibody was added to the supernatant and incubated overnight at 4°C. The immune complexes were collected as described and washed twice in dilution buffer and once in 1% β-mercaptoethanol. The washed immunoprecipitates were boiled for 5 min in 20 μl SDS sample buffer containing β-mercaptoethanol. These samples were counted by liquid scintillation and loaded onto a 17% SDS-polyacrylamide gel with prestained low molecular weight standards. After electrophoresis, the gels were fixed and treated as described elsewhere (Julius et al., 1984*a*).

Results

Double Mutants of myo2-66 and a Subset of Late-acting sec Genes Are Inviable at 25°C

Mutant alleles of genes which function on the same pathway or on parallel pathways often display synthetic effects in combination with each other. Many of the temperature-sensitive *sec* mutants blocked at the post-Golgi stage of the secretory pathway are inviable even at the permissive temperature when combined to generate haploid double *sec* mutants (Salminen and Novick, 1987). If the *MYO2* gene product is directly or indirectly involved in facilitating the transport of post-Golgi vesicles, one might predict that *MYO2* would exhibit interactions with genes required for secretion. Thus we initially examined double mutants between *myo2-66* and alleles of the early- and late-acting *sec* genes (Novick et al., 1980, 1981).

Crosses were made between *myo2-66* and representative alleles of ER-Golgi (early) *sec* genes and post-Golgi (late) *sec* genes. Diploids were sporulated at 25°C and 12–24 tetrads per cross were dissected and analyzed. In crosses with seven of the late-acting *sec* genes (*sec2-41*, *sec4-8*, *sec5-24*, *sec8-9*, *sec9-4*, *secl0-2*, and *secl5-1*), approximately one-fourth of the meiotic products were inviable at the permissive temperature. The pattern of temperature sensitivity among the viable progeny indicated that these *myo2-66*, *sec* double mutant combinations were lethal at 25°C (Table II). In tetrads with four viable spores (parental ditype) at 25°C, all were temperature sensitive. Tetrads containing three viable spores (tetratype) contained two which were temperature sensitive. In cases where only two spores were viable at 25°C (nonparental ditype), both were temperature resistant. In contrast, the combinations of *myo2-66* and the early-acting *sec* genes were clearly not synthetically lethal as seen by the pattern of spore viability. In all tetrads, four spores were viable at 25°C and the pattern of temperature sensitivity among these progeny indicated independent segregation of the *myo2-66* and *sec* mutations. Thus, *myo2-66* is synthetically lethal with *sec2-41*, *sec4-8*, *sec5-24*, *sec8-9*, *sec9-4*, *secl0-2*, and *secl5-1*. As shown in Table II, this subset of late-acting *sec* genes also genetically interacts with *sec4-8* (Salminen and Novick, 1987).

Previous work has shown that duplication of *SEC4* partially suppresses the temperature sensitivity of most of the *sec* mutants with which *sec4-8* is synthetically lethal (Salminen and Novick, 1987). Duplication of *SEC4* efficiently suppresses the *myo2-66* growth defect at 30°C and partially suppresses at 34°C (data not shown). Together, these data demonstrate that *myo2-66* genetically interacts with a subset of late-acting *SEC* genes, and suggests that the Myo2 protein may function at the post-Golgi stage of the secretory pathway or on a parallel pathway that shares many of the same components.

Table II. Summary of Viability of myo2-66, sec Double Mutants at 25°C*

ER-Golgi	*myo 2-66 x*	*sec 4-8 x*
sec 7-1	+	+
sec 12-4	+	+
sec 13-1	+	+
sec 14-3	+	+
sec 16-2	+	+
sec 17-1	+	+
sec 18-1	+	+
sec 19-1	+	+
sec 20-1	+	+
sec 22-3	+	+
Golgi-PM		
sec 1-1	+	+
sec 2-41	−	−
sec 3-2	+	+
sec 4-8	−	NA
sec 5-24	−	−
sec 6-4	+	+
sec 8-9	−	−
sec 9-4	−	+
sec 10-2	−	−
sec 15-2	−	−

* Strains were crossed at 25°C, diploids sporulated, and tetrads dissected and analyzed on YPD plates at 25°C.

myo2-66 Mutants Are Not Defective in the Processing or Transport of Invertase or α Factor

Previous studies have shown that the *myo2-66* mutation does not block the secretion of invertase at the restrictive temperature (Johnston et al., 1991). However, these studies did not test for the accumulation of an intracellular pool of invertase or for a kinetic lag in export. We examined the transit time of invertase secretion by pulse-chase analysis. In yeast, invertase is found as a constitutively expressed cytoplasmic protein and as a secreted glycoprotein regulated by hexose repression (Carlson and Botstein, 1982). The secreted protein undergoes core glycosylation in the ER followed by mannose extension in the Golgi to yield a mature high molecular weight species (Esmon et al., 1981) that is released into the periplasm of yeast cells. To detect invertase in immunoprecipitates, a high copy number plasmid bearing the *SUC2* gene which encodes invertase was introduced into *myo2-66* and wild-type strains. Pulse chase experiments on regenerated *myo2-66* spheroplasts revealed that the transit time for invertase is ~5 min, similar to that of wild-type spheroplasts (Fig. 1). At the 0-min time point after a 4-min pulse, all of the immunoprecipitated invertase was in its core glycosylated form and still within the cells for both mutant and wild-type samples. By two min of chase, some fully glycosylated invertase was found in the internal and external fraction of

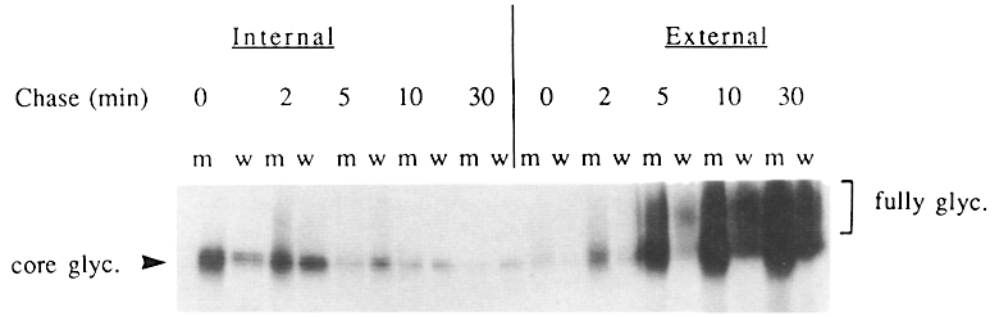

Figure 1. Kinetics of invertase secretion are equivalent in *myo2-66* and wild-type cells. Cells containing the *SUC2* gene on a high copy plasmid (NY 1031, *myo2-66*, and NY 1032, wild type) were first derepressed for invertase synthesis at 25°C, converted to spheroplasts, and then regenerated. The recovered spheroplasts were shifted to 37°C for 30 min, and then labeled with ^{35}S-*trans* label for 4 min at 37°C, and chased with 5 mM cysteine and methionine for 0, 2, 5, 10, and 30 min at 37°C. Cell aliquots were microcentrifuged at time points to separate the cells from the media, and both internal and external fractions were boiled in 1% SDS and immunoprecipitated with anti-invertase antibody as described in Materials and Methods. The washed immunoprecipitates were resuspended in SDS sample buffer, loaded on 10% SDS gels, and processed for autoradiography. Both strains (*m*, *myo2-66*, *w*, wild type) secrete fully processed invertase within 5 min of chase.

both mutant and wild-type strains. After 5 min of chase, most of the glycosylated invertase was found secreted into the external fraction in both *myo2-66* and wild-type samples. By 10 min of chase, all of the glycosylated invertase was found externally in both strains. As a control for cell lysis we have quantitated the cytoplasmic, unglycosylated form of invertase by scanning densitometry and found that less than 15% of it is found in the secreted fraction (data not shown). Furthermore, no other form of invertase was found within the cells, indicating that there was no internal accumulation of the secretory form of the protein or of any degradation products. This experiment clearly shows that newly synthesized invertase in *myo2-66* cells is efficiently transported into the periplasm with wild-type kinetics.

To address whether *myo2-66* cells are defective in the processing or export of a protein which is normally secreted into the media, we next examined the transport of the peptide pheromone α factor. The α factor mating pheromone is processed through the secretory pathway (Julius et al., 1984*a*), and its final modification occurs via the conversion of pro-α factor to mature α factor (a tridecapeptide) by peptidases in a late Golgi compartment (Julius et al., 1984*b*; Wilcox and Fuller, 1991). The pulse chase experiment in Fig. 2 shows that mature α factor is secreted from both wild-type and mutant cells within 5 min of chase after labeling for 8 min. Furthermore, although α factor is found associated with the cells at the initial zero time point, a significant amount is rapidly chased into the medium by 2 min. In addition, no other form of α factor is found accumulated within the cells (not shown). Thus, the α factor processing compartment is functional in *myo2-66* cells, and the secretion of α factor and invertase is unimpaired.

Transport of Major Glycoproteins Is Normal in myo2-66 Cells

To examine the fates of additional exported proteins in *myo2-66* cells, we studied the transport of several major secreted glycoproteins which bind to Con A. A pulse chase protocol was performed on regenerated wild-type and *myo2-66* spheroplasts, followed by Con A precipitation. Five major secreted glycoproteins (30, 35, 45, 116, and 200+ kD) were observed in both strains (Fig. 3). As Fig. 3 illustrates, wild-type (B) or *myo2-66* (A) cells show similar kinetics of glycoprotein transport out of the cell. While the 116-kD glycoprotein is secreted even at the 0-min chase time point (after a 5-min pulse), the 200+, 45, and 35 kD glycoproteins appear by 15 min of chase. Finally, the 30-kD glycoprotein is chased into the secreted fraction by 30 min. Recently a gene encoding a high copy suppressor of *myo2-66*, *SMY1*, has been identified and shown to have homology to kinesin (Lillie and Brown, 1992). We reasoned that if Smy1 functions as a microtubule-based motor to bypass a *myo2-66* defect, disrupting microtubules in a *myo2-66* mutant may cause an observable block in secretion. To address this possibility, we treated *myo2-66* cells with nocodazole during the Con A precipitation experiment. Samples processed in parallel for immunofluorescence showed that essentially all of the tubulin staining had disappeared in the nocodazole-treated cells (data not shown). Fig. 3 shows that *myo2-66* and wild-type strains exhibit similar kinetics of glycoprotein secretion whether treated with (+) or without (−) nocodazole. It

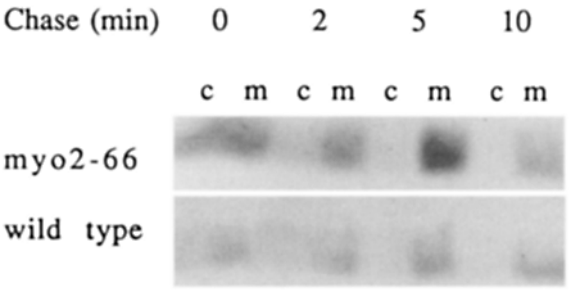

Figure 2. The secretion of mature α factor occurs with similar kinetics in wild-type and *myo2-66* cells. Cells (NY 1005, *myo2-66*, and NY 180, wt) were preshifted to 37°C for 30 min, and then labeled with ^{35}S-*trans* label for 8 min and chased with 10 mM cysteine and methionine for 0, 2, 5, and 10 min. At each time point, cells were separated from the media by brief centrifugation, samples were TCA precipitated, washed in acetone, lysed with glass beads, and immunoprecipitated with anti-α factor antibody as described in Materials and Methods. The washed immunoprecipitates were resuspended in SDS sample buffer and loaded onto a 17% SDS polyacrylamide gel and processed for autoradiography as described in Materials and Methods. Mature α factor is completely secreted from the cells (*c*) into the medium (*m*) by 5 min of chase in both *myo2-66* and wild-type cells shifted to 37°C.

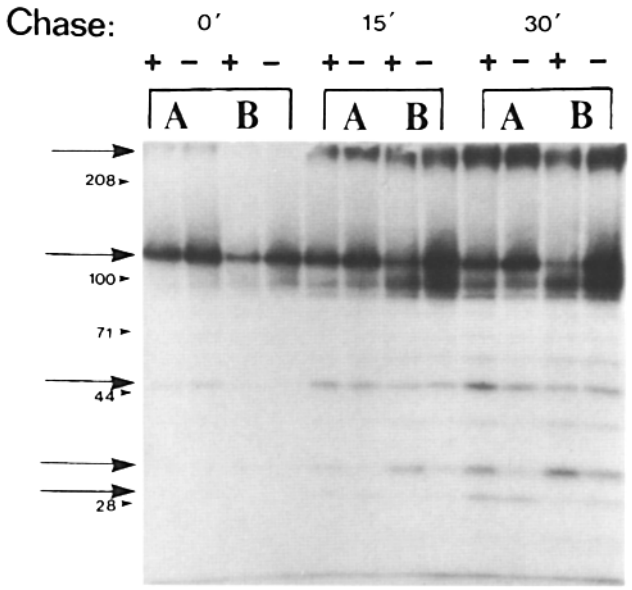

Figure 3. Glycoproteins are secreted normally from *myo2-66* cells, even after nocodazole treatment. Regenerated spheroplasts treated (+) with 15 μg nocodazole and 1% DMSO or mock-treated (−) with 1% DMSO were pulse labeled with ^{35}S-*trans* label for 5 min, and then chased for the times indicated. The cellular and media fractions were separated by microcentrifugation, and the media fraction was denatured by boiling in 1% SDS, and then precipitated with Con A Sepharose beads. The precipitates were washed, boiled in sample buffer, and loaded onto a 10% SDS polyacrylamide gel. The arrows indicate the appearance of the major secreted glycoproteins. All of these glycoproteins are transported out of the cell in both *myo2-66* (*A*) and wild-type (*B*) cells shifted to 37°C. Their approximate molecular masses are (*from top to bottom*): 200+, 116, 45, 35, and 30 kD.

seems that the 35-kD glycoprotein is more evident in the nocodazole-treated cells at the 15-min chase time point in both mutant and wild-type samples. A similar nocodazole treatment was applied to samples in the invertase pulse-chase experiment described in Fig. 1. In this case also, nocodazole did not affect the kinetics of invertase secretion in *myo2-66* cells (not shown).

Eleven major proteins are found on the yeast cell surface, and most of these bind to Con A (Novick and Schekman, 1983). It has previously been shown that secretory mutants are defective in the transport of all of these major cell surface glycoproteins (Novick and Schekman, 1983). We conducted pulse chase experiments on regenerated spheroplasts followed by protease protection and Con A precipitations to examine the pathway of glycoprotein transport to the cell surface in *myo2-66* and wild-type cells. From these pulse-chase/protease protection studies, we determined that the same set of four glycoproteins (roughly 30, 50, 80, and 200+ kD in size) reached the cell surface and became protease-sensitive with the same kinetics in both *myo2-66* and wild-type cells (data not shown). The pattern of protease-resistant bands was also found to be identical in both strains (not shown). Thus, a number of different membrane-bound and secreted proteins are correctly processed and delivered normally in *myo2-66* mutants, even under conditions of microtubule disruption.

Since the plasma membrane ATPase accumulates in secretory vesicles found in late-acting *sec* mutants (Walworth and Novick, 1987), we sought to determine if this protein was associated with vesicles in *myo2-66* cells. Through immunofluorescence staining, pulse chase experiments, and column fractionation, we found that the plasma membrane ATPase of *myo2-66* cells is correctly distributed on the yeast cell surface, is stable, and is not found on vesicles (data not shown).

Vacuolar Transport Is Not Defective in myo2-66 Mutants

Since transport to the cell surface and out of the cell seemed to occur normally in *myo2-66* cells, we next examined whether transport from the Golgi to the vacuole is impaired in the *myo2-66* mutant. It has recently been shown (Raymond et al., 1992; Vida et al., 1993) that the transport of vacuolar proteins is directed from the Golgi complex via a prevacuolar compartment (or endosome) to the vacuole. Since the delivery of soluble and membrane-bound vacuolar proteins is thought to occur by somewhat different mechanisms (Klionsky and Emr, 1989), we chose to study the transport of a representative protein from each class.

The soluble vacuolar protease carboxypeptidase Y (CPY) undergoes modifications in the ER and Golgi before arriving in the vacuole where it is cleaved by the *PEP4* gene product to its mature 61-kD active form. The ER (67 kD) form or Golgi (69 kD) form accumulate in mutants which are blocked at these stages of the secretory pathway (Stevens et al., 1982; Franzusoff and Schekman, 1989). Pulse chase studies on whole cell lysates indicated that the transit time for CPY processing and transport was similar to wild type in *myo2-66* mutants (Fig. 4). By 2 min of chase, the ER (*p1*) form of CPY was partially chased into the Golgi (*p2*) and the mature (*m*) form in both the mutant and in wild-type cells. By 5 min of chase, CPY was completely in its mature vacuolar form in both strains. Furthermore, by immunoblot analysis, CPY was not inappropriately secreted from *myo2-66* cells (data not shown).

Alkaline phosphatase (ALP) is an integral membrane glycoprotein of the yeast vacuole (Klionsky and Emr, 1989; Kaneko et al., 1987). ALP is processed from an inactive

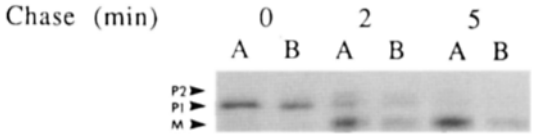

Figure 4. The soluble vacuolar protease carboxypeptidase Y (CPY) is processed and transported normally in *myo2-66* mutants. Cells (NY 1006, *myo2-66*, and NY 1033, wt) were shifted to 37°C for 30 min, and then were pulse labeled for 2 min with ^{35}S-*trans* label and chased with 10 mM cysteine and methionine for the times indicated. At each time point, cells were washed into 10 mM NaN_3 and lysed with glass beads. The samples were immunoprecipitated with anti-CPY antibody as described in Materials and Methods. The final washed, solubilized precipitates were loaded onto 8% SDS gels and processed for autoradiography. The ER precursor form of CPY (*p1* = 67 kD) is found in both *myo2-66* (*A*) and wild-type (*B*) samples at the zero time point, and then it is partially chased into the Golgi form (*p2* = 69 kD) and mature form (*m* = 61 kD) by 2 min in both strains. All of the CPY is in its mature, vacuolar form by 5 min in both strains.

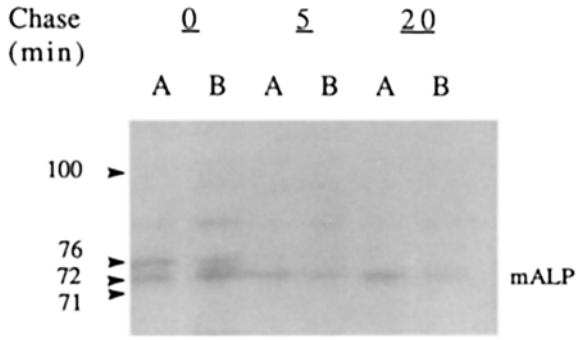

Figure 5. Alkaline phosphatase (ALP) is processed and delivered to the vacuole normally in *myo2-66* and wild-type cells. Cells (NY 1005, *myo2-66*, and NY 180, wt) were pulse labeled with ^{35}S-*trans* label for 5 min and chased with 10 mM cysteine and methionine for 0, 5, and 20 min as described in Fig. 3. The washed, solubilized precipitates were loaded onto 10% gels and processed for autoradiography. Within 5 min of chase, the precursor form (76 kD) of ALP is converted to the mature 72-kD vacuolar form in both wild-type (*B*) and *myo2-66* (*A*) cells.

precursor of 76 kD to a mature enzyme of 72 kD upon reaching the vacuole. Klionsky and Emr (1989) proposed that ALP may differ somewhat from CPY in its final targeting to the vacuole. To examine this transport pathway, whole cells were pulse labeled and immunoprecipitated with anti-ALP antibody. In both mutant and wild-type cells, the precursor form of ALP was converted to the mature 72-kD enzyme within 5 min of chase after a 5-min pulse (Fig. 5). Therefore, both a membrane-bound and a soluble vacuolar protein are processed and transported efficiently in *myo2-66* mutants.

myo2-66 Cells Are Not Defective in the Transport or Internalization of the a-Factor Receptor

Since we found that neither the secretory pathway nor the vacuolar transport pathway are slowed or disrupted in *myo2-66* cells, we sought to determine if endocytosis or transport of a membrane receptor is affected in this mutant. It has recently been shown that *myo2-66* mutants are not defective in the uptake of labeled α factor (Kubler et al., 1994), indicating that they do not exhibit a defect in receptor-mediated endocytosis. Therefore we examined the transport and constitutive endocytosis of the a-factor receptor. This receptor is normally found on the surface of α cells where it functions to bind the a-factor mating pheromone and induce the mating response. The a-factor receptor undergoes internalization after a transient association with the cell surface, and is delivered to the vacuole via endosome-like structures (Davis et al., 1993). Once it reaches the vacuole, the receptor is degraded by the *PEP4* gene product. To follow the a-factor receptor as it is brought to the cell surface, and then retrieved back into the cell, we employed the protocol described by Davis et al. (1993). *PEP4* deficient *MYO2* and *myo2-66* strains were pulse labeled and chased as described (see Materials and Methods) and before spheroplasting, the cells were treated with and without protease to degrade any a-factor receptor at the cell surface. We found that the transport of newly synthesized a-factor receptor to the cell surface in *myo2-66* mutants occurred at rates similar to wild-type cells, as a portion of the labeled receptor became accessible to exogenous protease within 10 min of chase after a 10-min labeling period (Fig. 6). However, from the amount of full-length receptor observed at the 10-min chase time (Fig. 6), it appears that the amount of receptor that becomes protease sensitive in the mutant is somewhat reduced compared to wild type. Protease sensitivity of the receptor was also confirmed by the appearance of a 30-kD digestion product at the 10-min chase time point (Fig. 6). The a-factor receptor became largely inaccessible to protease by 30 min of chase in the *myo2-66* mutant, as indicated by the absence of the 30-kD digestion product and the increase in the abundance of the full-length protein by 30 min. In contrast, the full-length protein was still reduced in abundance at 30 min of chase in wild-type cells and the 30-kD proteolytic fragments persisted through 90 min of chase. These results demonstrate that a large fraction of a-factor receptor does reach the cell surface by 10 min in both the mutant and wild-type strains. However, a pool of receptor may either fail to reach the surface in the *myo2-66* cells or it may reach the surface and become rapidly internalized by 10 min of chase. A block in receptor export should result in an increased vesicular pool of a-factor receptor in *myo2-66* cells. However, no such vesicular pool of a-factor receptor was found in fractionation

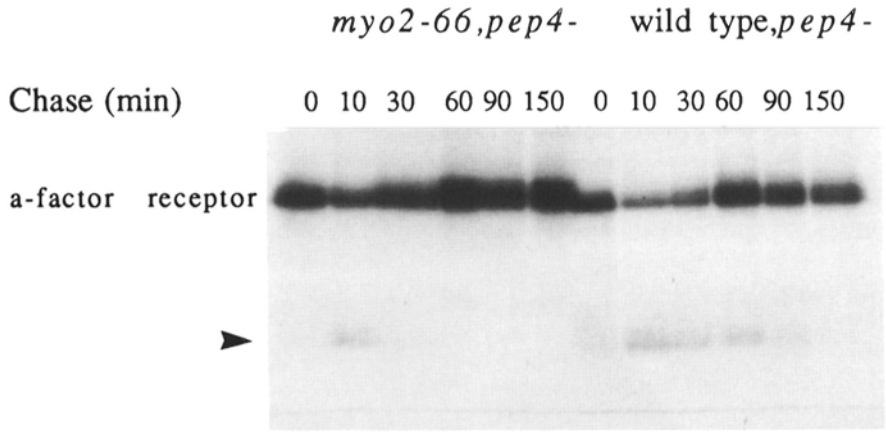

Figure 6. Surface accessibility of the a-factor receptor in *myo2-66,pep4::URA3* cells. *Mat* α, *PEP4* deficient, wild-type (NY 579) or *myo2-66* (NY 1125) cells were shifted to 30°C for 30 min, and then pulse labeled for 10 min with ^{35}S in vitro labeling mix, chased with 10 mM cysteine and methionine for 0, 10, 30, 60, 90, and 150 min, washed into 10 mM KF and NaN_3 on ice and digested with 1 mg/ml Pronase E for 1 h at 37°C before spheroplasting and lysis. Both mutant and wild-type strains show the receptor protected from protease at zero min, but then at 10 min of chase the receptor band diminishes, while a 30-kD proteolytic fragment appears (*arrow*), indicating that the receptor has reached the cell surface. The receptor then becomes internalized into a protease-protected compartment by 30 min in the mutant strain as evidenced by the absence of the degradation product, while in wild-type cells a portion of the 30-kD fragment persists even at 90 min of chase.

experiments of *myo2-66* lysates (not shown). In addition, we have observed that the a-factor receptor appears to be internalized more completely in the *myo2-66* mutant (Fig. 6).

myo2-66 Mutants Accumulate Vesicles Predominantly in the Mother Cell upon Short Incubations at 37°C

Wild-type yeast cells (Fig. 7 *a*) contain very few secretory vesicles within their cytoplasm, as vesicle turnover is rapid. Johnston et al. (1991) have shown that in *myo2-66* mutants, 80–100 nm vesicles accumulate throughout the cell after a 3-h shift to the nonpermissive temperature. To understand the origin and destination of these vesicles, we characterized the vesicle-accumulation phenotype of *myo2-66* cells as a function of time and cell polarity through an electron microscopic study performed on cells synchronized at the small budded stage. Mating type "a" cultures were arrested with α factor at the unbudded stage of the cell cycle, and then small

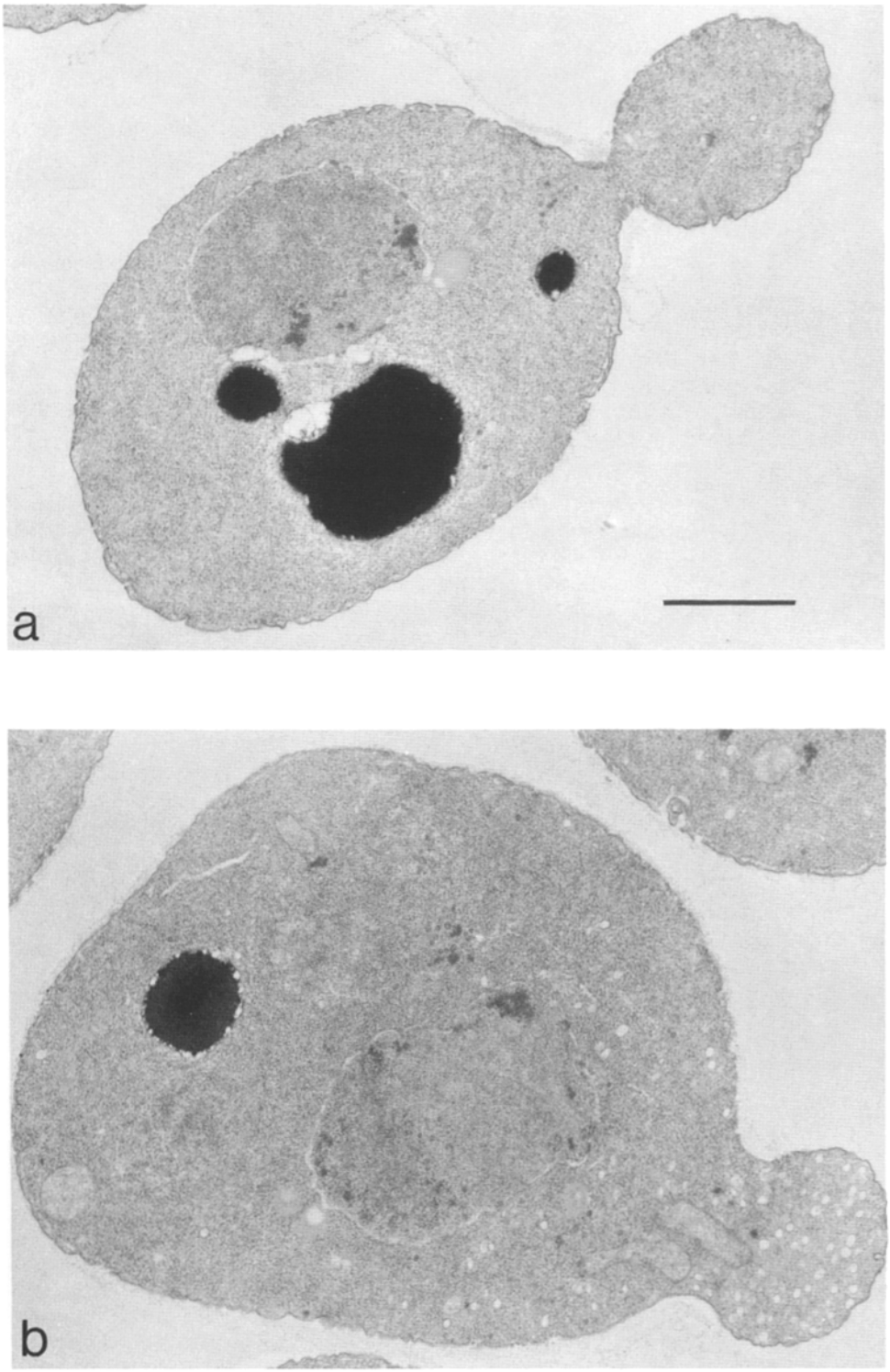

Figure 7. Electron microscopy of wild-type or *sec6-4* cells shifted to 37°C for 10 min. Cells were prepared for TEM as described in Materials and Methods. *a* is a representative wild-type cell (NY 13) which does not accumulate secretory vesicles, and *b* is a typical *sec6-4* (NY 17) cell showing vesicle accumulation mainly in the bud. Bar, 1 μm.

buds were allowed to form in fresh medium at the permissive temperature. Cells were then shifted to 37°C for 0, 10, or 20 min, and subsequently fixed and sectioned for TEM (see Materials and Methods).

In two post-Golgi *sec* mutants, *sec1-1* and *sec6-4*, upon a short incubation at the nonpermissive temperature, secretory vesicles accumulated within the bud of the cell (Fig. 7 *b*). These cells showed a quantitative increase in both vesicle number and vesicle density in the bud up until 15 min at 37°C (Fig. 10 *A*). After this time point, the vesicle density in the mother cell (mainly the neck region) began to increase as the bud was saturated (Fig. 10 *B*). This reflects the inability of these vesicles to fuse with the plasma membrane of the bud. In contrast, *myo2-66* cells shifted to 37°C for 10 min accumulated vesicles almost exclusively in the mother cell (Fig. 8 *b*). Even at the permissive temperature (0 min) *myo2-66* cells showed some vesicle accumulation within the cytoplasm of the mother cell and few vesicles in the bud (Fig. 8 *a*). After 20 min (Fig. 8 *c*) at the restrictive temperature, *myo2-66* mutant cells continued to show increased vesicle accumulation predominantly in the mother cell while few vesicles were found in the bud. Quantitation of vesicle accumulation in *myo2-66* cells confirmed that the number and density of vesicles in the mother cell increased linearly with time (Fig. 10 *B*), while staying constant, and low in number, in the bud (Fig. 10 *A*). This phenotype of *myo2-66* cells indicates a defect in the transport and/or fusion of vesicles with their correct target membrane and may reflect a block in vesicle transport into the bud.

EM of Double Mutants

Phenotypic analysis of double mutants can establish epistatic relationships (Huffaker et al., 1988; Kaiser and Schekman, 1990; Novick et al., 1981). We first sought to identify the relationship of *MYO2* function with respect to the function of three different classes of *SEC* genes: those involved in ER to Golgi, intra-Golgi, or post-Golgi transport. Since the EM phenotype of the various *sec* mutants is clearly distinct from the *myo2-66* phenotype, we were able to establish the relationships between several of these gene functions by performing EM analysis on various double mutants.

If *MYO2* functions in a *SEC*-dependent pathway, a double mutant should exhibit a phenotype reflecting the earlier block. A *myo2-66, sec6-4* double mutant was initially examined. *sec6-4* mutants accumulated post-Golgi secretory vesicles in the bud when shifted to the restrictive temperature (Fig. 7 *b*). In contrast, the *myo2-66, sec6-4* double mutant accumulated vesicles in the mother cell (Fig. 9 *a*), as did the *myo2-66* single mutant (Fig. 9 *b*). The quantitation of vesicle density in the mother and bud of the *myo2-66, sec6-4* mutant was similar to the *myo2-66* single mutant in that vesicle accumulation in the mother cell increased with time but remained constant in the bud (Fig. 10, *A* and *B* and Table III). Thus, by this criteria alone, *MYO2* appears to function before *SEC6*. However, unlike the *myo2-66* mutant, the *myo2-66, sec6-4* double mutant displays the same tight block in invertase secretion as the *sec6-4* mutant alone (data not shown). Thus *myo2-66* does not bypass a *SEC6*-requiring step in the secretory pathway. Taken together, the EM phenotype combined with the assay for internal invertase in the double mutant shows that this double mutant exhibits some phenotypic characteristics of each single mutant.

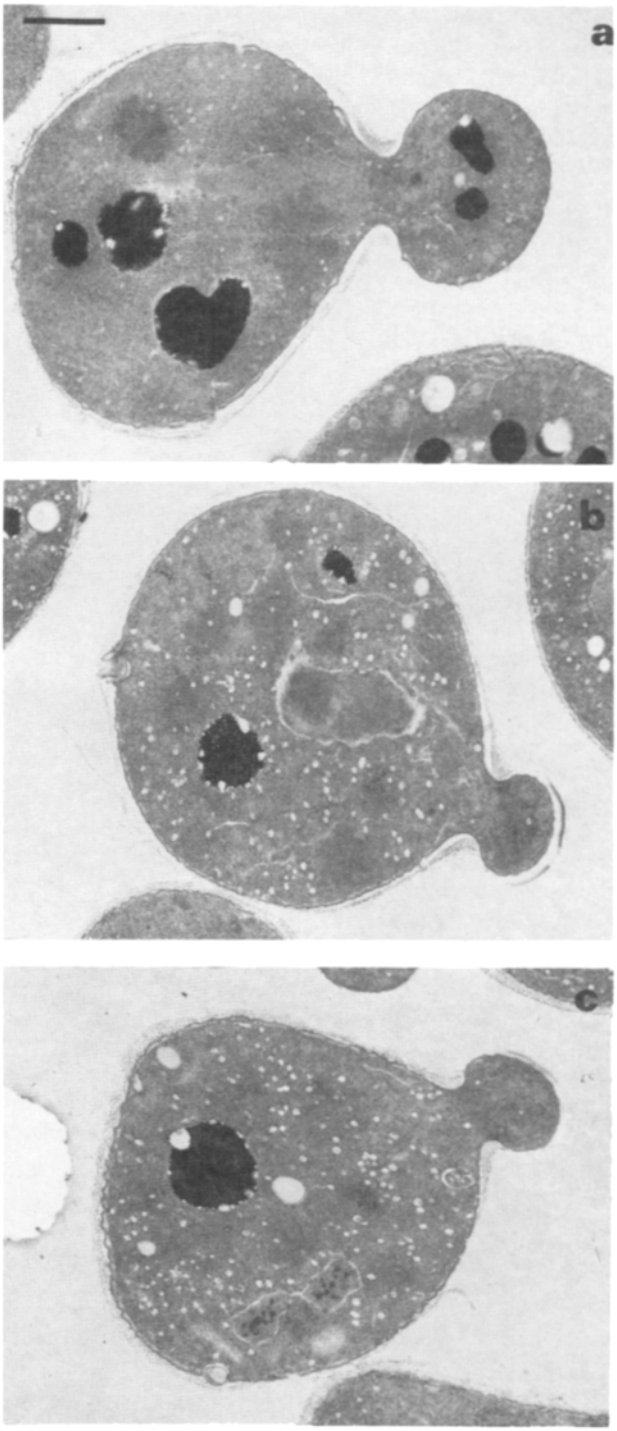

Figure 8. Time course of *myo2-66* cells shifted to 37°C for short periods. Cells (NY 829) were synchronized with α factor, released from G1 arrest, and allowed to form small buds at 25°C, and then incubated at 37°C for the following times (*a*) 0 min, (*b*) 10 min, and (*c*) 20 min. At the various time points, cells were fixed for TEM. Vesicle accumulation occurs predominantly in the mother cell with time, while few vesicles appear in the bud. Bar, 1 μm.

To define the *myo2-66* block with respect to other landmarks on the secretory pathway, double mutants in which *myo2-66* was combined with ER to Golgi blocked *sec* alleles were examined. *SEC13* facilitates ER to Golgi transport by catalyzing the budding of carrier vesicles (Salama et al.,

1993), and *sec13-1* mutant cells accumulate only ER membranes at the restrictive temperature. Double mutant, *sec13-1, myo2-66*, cells displayed the same morphological phenotype as the *sec13-1* single mutant (Fig. 9 *b*). *SEC18* is also required for transport between the ER and Golgi complex, catalyzing the fusion of carrier vesicles (Rexach and Schekman, 1991; Graham and Emr, 1991). A *sec18-1* mutant builds up ER membranes and small (50 nm) ER-derived transport vesicles at the restrictive temperature (Novick et al., 1981). Double mutant, *myo2-66, sec18-1*, cells also accumulated ER membranes and some small vesicles at the nonpermissive temperature (Fig. 9 *d*). Thus, Sec13 and Sec18

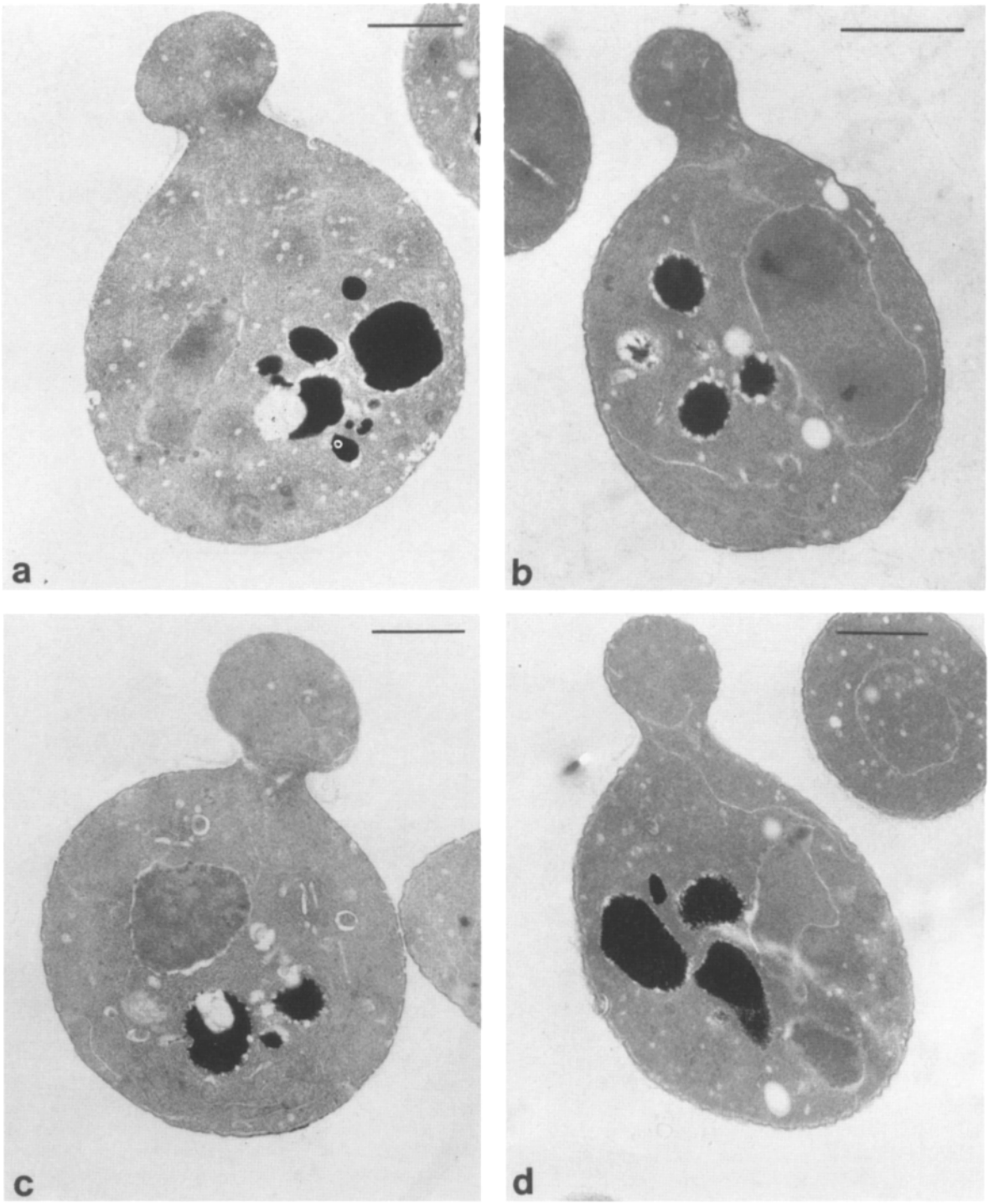

Figure 9. Electron microscopy of double mutants between *myo2-66* and representative *sec* mutants after 10 min at 37°C. Double mutants were constructed and prepared for TEM as described in Materials and Methods. (*a*) *myo2-66,sec6-4* (NY 895) accumulates vesicles predominantly in the mother cell, as seen in the *myo2-66* single mutant. (*b*) *myo2-66,sec13-1* (NY 922) accumulates only ER membrane as observed in the *sec13-1* single mutant. (*c*) *myo2-66,sec7-1* (NY 919) accumulates Golgi membranes as does the *sec7-1* single mutant. (*d*) *myo2-66,sec18-1* (NY 896) accumulates both ER-derived vesicles and ER membrane as does the *sec18-1* single mutant. Bar, 1 μm.

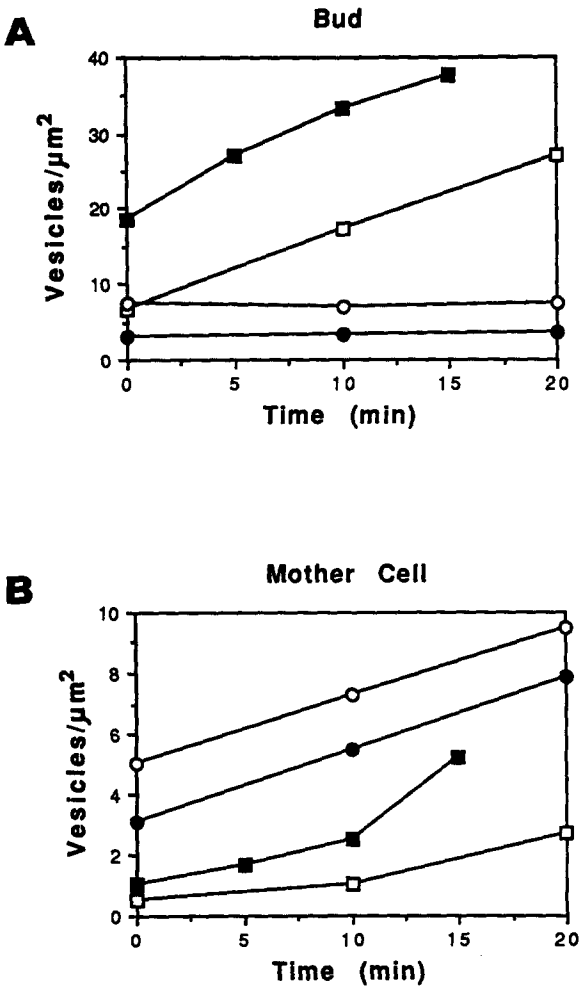

Figure 10. Quantitation of vesicle accumulation in the bud (*A*) and mother cell (*B*) of *sec6-4*, *sec1-1*, *myo2-66*, and {*myo2-66,sec6-4*} cells. Vesicle density was determined as described in Materials and Methods. In *sec1-1* (*open square*) and *sec6-4* (*filled square*) cells, vesicles accumulate in the bud linearly with time, whereas in *myo2-66* mutants (*open circle*), vesicle accumulation occurs preferentially in the mother cell with time, and the vesicle number and density in the bud remains low. The *myo2-66,sec6-4* double mutant (*filled circle*) exhibits the same vesicle density profile as the *myo2-66* single mutant.

must be active in order to generate the vesicles found in *myo2-66* cells.

Next, a *sec7-1*, *myo2-66* double mutant was examined. *SEC7* is involved in intra-Golgi transport and possibly ER-Golgi transport (Franzusoff and Schekman, 1989; Franzusoff et al., 1991). At the nonpermissive temperature *sec7-1* mutant cells accumulate Golgi membranes which are not readily observed in wild-type yeast cells by usual fixation methods. *sec7-1*, *myo2-66* double mutant cells shifted to 37°C also exhibited the characteristic Golgi stacks of the *sec7-1* mutant (Fig. 9 *c*). Therefore, *myo2-66* appears to block after *sec7-1*, and Sec7 function is required to form *myo2-66* vesicles.

Finally, to determine whether the vesicles in the *myo2-66* mutant could be derived from an endocytic or recycling pathway, we constructed double mutants of *myo2-66* with representatives from two stages of the endocytic pathway.

Table III. Vesicle Accumulation in myo2-66 and sec6-4 Mutants at 37°C*

Strain	Time at 37°C	Density		Average number of vesicles	
		Bud	Mother	Bud	Mother
	min	*(vesicles/μm²)*			
sec1-1	0	6.6 ± 5.0	0.5 ± 0.2	12.2	5.6
	10	17.2 ± 5.5	1.0 ± 0.3	46.0	12.9
	20	27.2 ± 8.0	2.7 ± 0.9	46.0	40.7
sec6-4	0	18.6 ± 8.9	1.0 ± 0.4	21.1	10.4
	5	27.2 ± 8.6	1.7 ± 1.0	48.1	20.6
	10	33.4 ± 10.4	2.5 ± 1.1	59.3	32.3
	15	37.8 ± 9.8	5.2 ± 1.4	59.0	60.1
myo2-66	0	7.5 ± 2.2	5.0 ± 2.1	17.0	67.0
	10	6.9 ± 2.3	7.3 ± 1.9	16.0	104
	20	7.5 ± 2.3	9.5 ± 2.2	16.0	137
myo2,sec6	0	3.2 ± 2.4	3.1 ± 2.7	9.0	47.0
	10	3.3 ± 2.3	5.5 ± 2.2	8.3	80.0
	20	3.5 ± 2.3	7.9 ± 2.7	9.8	114

* The density and number of vesicles located in both the bud and mother cell of *sec1-1*, *sec6-4*, *myo2-66*, and {*myo2-66,sec6-4*} cells after brief incubations at 37°C. Vesicle density was determined by dividing the number of vesicles within a particular region of the cell (bud or mother) by the corresponding area. Each value is the average of measurements made on 25–30 individual cells from 1–3 independent experiments ±SD.

REN1 functions in a late stage of endocytosis, possibly in transport from the endosome to the vacuole (Davis et al., 1993). *myo2-66/ren1*Δ double mutants still accumulate vesicles at the restrictive temperature (data not shown). Since the *ren*Δ cells alone do not accumulate any organelles (not shown), the vesicles in *myo2-66* cells are not derived from an endosome-to-vacuole pathway. *END4* encodes a protein which functions in the internalization step of endocytosis (Raths et al., 1993). We reasoned that if Myo2 acts in transporting endocytic or recycling vesicles, blocking internalization should prevent the accumulation of such vesicles. A *myo2-66/end4*Δ double mutant was constructed and shifted to 37°C for 2 h, along with the respective single mutants. Fig. 11 shows that like the *myo2-66* single mutant (*B*), the *myo2-66/end4*Δ double mutant (*C*) still accumulates vesicles within its cytoplasm. It should be noted that the numbers of vesicles in the single and double mutants are variable, possibly due to the heterogenous cell populations. It is clear, however, that preventing the internalization step of endocytosis does not block vesicle formation in *myo2-66* mutants.

Taken together, our EM studies indicate that Myo2 functions in a post-Golgi, *SEC*-dependent transport pathway with a terminal phenotype before *sec6-4*, but after that of *sec13-1*, *sec18-1*, and *sec7-1*. We have also ruled out the possiblity that the vesicles in the *myo2-66* mutant could be derived from an endocytic pathway, since blocking endocytosis does not prevent vesicle accumulation in these cells. From the EM data alone, the vesicles in the *myo2-66* mutants appear to be intermediates of the post-Golgi secretory pathway. Several models are considered below to account for the various lines of evidence concerning the cellular function of the Myo2 protein.

Discussion

We have presented further characterization of the *myo2-66* mutant, and investigated the possible role of Myo2 in various

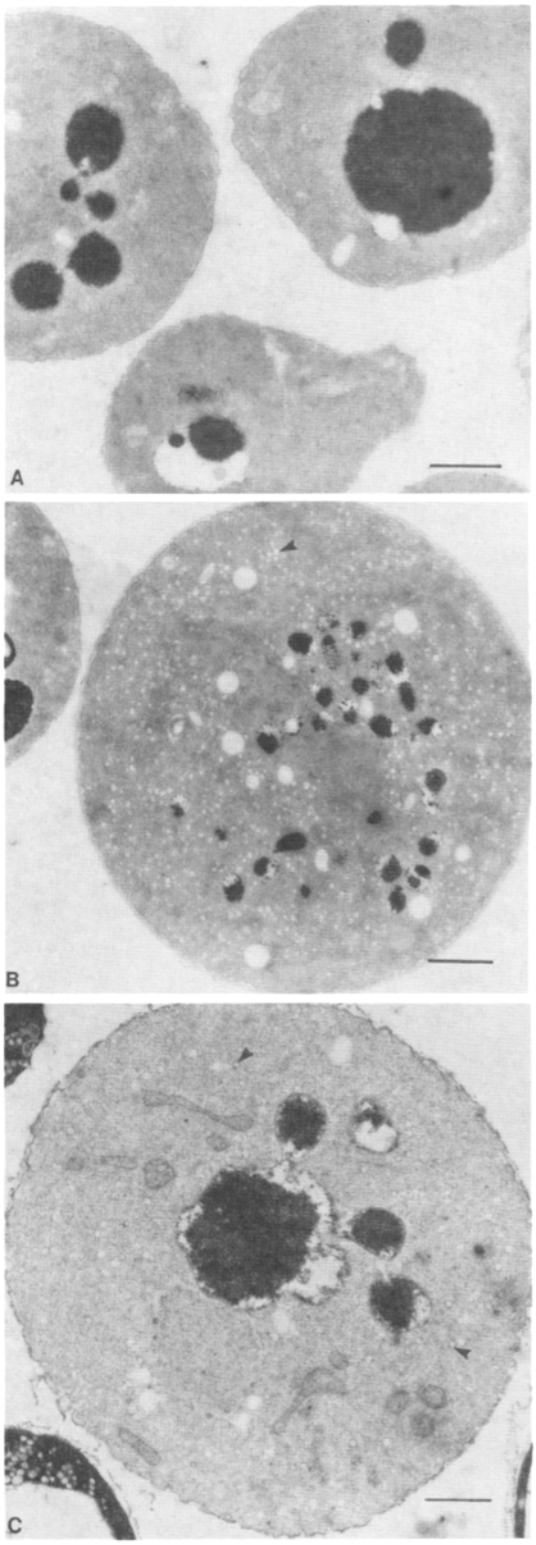

Figure 11. Electron microscopy of a *myo2-66/end4Δ* double mutant after 2 h at 37°C. Double mutants of *myo2-66* and *end4::LEU2* were constructed and confirmed by complementation. Single or double mutant cells were shifted to 37°C for 2 h, and then fixed and processed for TEM. (*A*) *end4Δ* cells (NY 1180) alone do not accumulate any organelles within their cytoplasm. (*B*) *myo2-66* cells (NY 1005) accumulate many vesicles (*arrow*) within their cytoplasm. (*C*) *myo2-66,end4::LEU2* double mutants (NY 1235) also accumulate vesicles (*arrows*) within their cytoplasm. The degree of vesicle accumulation among *B* and *C* is somewhat variable, perhaps due to the asynchronous cell populations. Bar, 1 μm.

vesicular transport pathways. First, we examined the genetic interactions of this mutation with known *sec* mutations, and found that *myo2-66* displays synthetic lethality with a subset of post-Golgi blocked *sec* mutations, but not with any mutations which act earlier in the secretory pathway. These interactions suggest that Myo2 functions on a pathway that also requires the late-acting *SEC* gene products. We can therefore speculate that Myo2 facilitates a transport pathway that involves fusion of vesicles with the plasma membrane, and not in transport from the ER to the Golgi complex. Liu and Bretscher (1992) have reported that *myo2-66* is synthetically lethal with a disruption of the yeast tropomyosin gene, *TPM1*, and since the mutant phenotype of *TPM1* disrupted cells is very similar to *myo2-66* mutants (Liu and Bretscher, 1992), the two genes may be involved in concerted functions.

The *myo2-66* mutant was previously shown to accumulate vesicles within its cytoplasm upon a 3-h shift to the restrictive temperature. We have observed that upon short shifts to 37°C, vesicles accumulate predominantly in the mother cell, and not in the bud of *myo2-66* cells. This is in contrast to the pattern we observed in late-acting *sec* mutants, such as *sec6-4* and *sec1-1*, in which vesicles are found predominantly in the bud after brief incubations at the restrictive temperature. In the case of *sec6-4* and *sec1-1*, post-Golgi secretory vesicles reach the bud, but are unable to fuse with its plasma membrane. In the *myo2-66* mutant, however, vesicle accumulation in the mother cell may reflect a targeting or delivery defect, and this is consistent with a model in which Myo2 acts as a motor to move vesicles from the mother cell into the bud. Alternatively, it may reflect a defect in segregating components of the secretory apparatus, such as the Golgi complex, into the bud. Analogous phenotypes have been observed in *dilute* mice and *unc-104* mutants of *C. elegans*. In the case of *dilute*, loss of function of this class V myosin leads to a defect in the transport of pigment granules in melanocytes (Mercer et al., 1991). In the case of *unc-104*, the defect in this kinesin-related gene product causes the accumulation of synaptic vesicles specifically in the neuronal cell bodies due to a failure in anterograde axonal transport (Hall and Hedgecock, 1991).

Even though *myo2-66* cells rapidly accumulate vesicles, previous studies demonstrated that bulk secretion still continues in these cells, although perhaps in a nonpolarized fashion. The appearance of vesicles without a concomitant block in protein export led to the proposal that secretion continues because secretory vesicles make their way to the cell surface more slowly in the *myo2-66* mutant (Johnston et al., 1991). This hypothesis would predict a kinetic lag in the transport of secretory proteins. We have shown, however, that there is no detectable lag in the transport of a number of secreted, cell surface or vacuolar proteins in *myo2-66* cells. It is possible that secretory proteins accumulate in *myo2-66* vesicles, but get degraded. However, in our pulse-chase experiments, we have not observed any degradation products or internal intermediates. It should be noted that after a shift to 37°C, wild-type cells mislocalize actin (by immunofluorescence) for up to 60 min. It is possible that Myo2 might normally act to speed vesicular transport, but the loss of actin polarity resulting from the temperature shift masks this effect. However, a temperature shift does not, by itself, slow secretion or result in the accumulation of vesicles. The efficient vesicular transport seen in wild-type cells after a temperature shift presumably reflects the presence of resid-

ual actin structures that are not detected by immunofluorescence, since temperature sensitive actin mutants do exhibit a partial block in secretion as well as vesicle accumulation.

The absence of a secretory block in *myo2-66* cells might indicate that vesicles can use an alternate cytoskeletal track and motor to move into the bud. This is an appealing proposal since a kinesin-like suppressor of *myo2-66* has been identified (Lillie and Brown, 1992). In squid axoplasm, crosstalk between microtubule-based and actin-based transport mechanisms has been observed; vesicles were found to switch from moving along microtubules to actin filaments sequentially (Kuznetsov et al., 1992). In addition, Golgi-derived vesicles in the brush border possess both dynein and myosin-I, suggesting that a vesicle can use more than one cytoskeletal track (Fath et al., 1994). However, we found that disrupting microtubules with nocodazole in *myo2-66* cells does not lead to a tighter block in invertase or glycoprotein secretion. This suggests that Myo2 does not operate in parallel with a microtubule-based transport system.

One could postulate that the *myo2-66* vesicles contain a specific subset of secretory proteins that are as yet unidentified, and in a recent review, Bretscher et al. put forth a similar proposal to resolve the surprising observation of vesicle accumulation without concomitant secretory defects in both *myo2-66* and *tpm1* mutants (Bretscher et al., 1994). It is possible that Myo2 and Tpm1 both function on a pathway that requires the late *SEC* gene products, but which facilitates the transport of a specific class of proteins. Since *myo2-66* was originally identified as a cell cycle mutant, *cdc66-1* (Johnston, 1991), it may be that the vesicles which accumulate in this mutant contain cargo needed for a particular stage of the cell cycle. The cargo of the *myo2-66* vesicles could be components necessary for cell wall assembly, such as chitin synthetases, chitinase, or endoglucanases. Alternatively, they could ferry proteins needed for mating (e.g., Fus1). Once a marker for purifying these vesicles is found, analysis of the composition and cargo of the vesicles should be enlightening. Recently, two classes of post-Golgi secretory vesicles have been identified in a late-acting *sec* mutant (Harsay, E., and A. Bretscher. 1994. *Mol. Biol. Cell.* 5:443a). If Myo2 were required for transport of only one set of vesicles, then the other set should still accumulate in the bud of the *myo2-66, sec6-4* double mutant. However, our EM analysis of the double mutant indicates that there is no large class of vesicles transported to the bud in a Myo2 independent fashion. Perhaps the invertase-containing vesicles represent only a minor pool of the total post-Golgi vesicles. Another possible model is that Myo2 is required to move both types of vesicles into the bud. The subset of vesicles which accumulate in *myo2-66* cells must be targeted to the bud in order to fuse, while the invertase-containing vesicles can fuse equally well with the plasma membrane of the mother cell. This model is consistent with the very large mother cells seen in *myo2-66* cultures.

The Myo2 protein is found predominantly at the tip of the bud in wild-type yeast (Lillie and Brown, 1994) and along with calmodulin and actin, it changes its distribution throughout the cell cycle to regions of active growth (Brockerhoff et al., 1994). This localization may reflect the destination of a Myo2-dependent transport pathway involved in establishing and maintaining polarized growth. However, we must also consider other, less direct, roles for Myo2 in vesicular transport. An alternate function of Myo2 may be to organize polarized growth at the cell surface by recruiting components required for bud assembly and growth. Myo2 may facilitate the polarized distribution of these bud site proteins by organizing the actin cytoskeleton. Finally, Myo2 may also act to support the dynamic changes of the actin-plasma membrane interface in facilitating cell wall growth (see Mulholland et al., 1994). To sort out these possible avenues of Myo2 function, it will be important to determine if Myo2 functions on the surface of the vesicles and/or at the plasma membrane.

We would like to thank Dr. G. Johnston for the *myo2-66* strain. We would also like to thank the following for their generous gifts of antibodies: Drs. N. Davis and G. Sprague (anti a-factor receptor), Dr. T. Stevens (alkaline phosphatase), Dr. S. Ferro-Novick (invertase and α factor), and Dr. P. Brennwald (carboxypeptidase Y). We are grateful to Dr. N. Davis and Dr. S. Brown for sharing results before publication. We would like to thank Drs. R. Cheney, R. Collins, and M. Mooseker for their critical reading of the manuscript, H. Tan for his assistance in photography, and L. Vanacore for her assistance in thin section electron microscopy.

This work was supported by grants to P. Novick from the National Institutes of Health (GM35370) and the Donaghue Foundation. B. Govindan and R. Bowser were supported by predoctoral training grants.

Received for publication 10 October 1994 and in revised form 20 December 1994.

References

Adams, A. E. M., and J. R. Pringle. 1984. Relationship of actin and tubulin distribution to bud growth in wild-type and morphogenetic-mutant *Saccharomyces cerevisiae*. *J. Cell Biol.* 98:934–945.

Amatruda, J. F., J. F. Cannon, K. Tatchell, C. Hug, and J. A. Cooper. 1990. Disruption of the actin cytoskeleton in yeast capping protein mutants. *Nature (Lond.).* 344:352–354.

Bretscher, A., B. Drees, E. Harsay, D. Schott, and T. Wang. 1994. What are the basic functions of microfilaments? Insights from studies in budding yeast. *J. Cell Biol.* 126:821–825.

Brockerhoff, S. E., R. C. Stevens, and T. N. Davis. 1994. The unconventional myosin, Myo2p, is a calmodulin target at sites of cell growth in *Saccharomyces cerevisiae*. *J. Cell Biol.* 124:315–323.

Brown, S. S. 1993. Phenotypes of cytoskeletal mutants. *Curr. Opin. Cell Biol.* 5:129–134.

Carlson, M., and D. Botstein. 1982. Two differentially regulated mRNAs with different 5′ ends encode secreted and intracellular forms of yeast invertase. *Cell.* 28:145–154.

Cheney, R. E., and M. S. Mooseker. 1992. Unconventional myosins. *Curr. Opin. Cell Biol.* 4:27–35.

Cheney, R. E., M. K. O'Shea, J. E. Heuser, M. V. Coelho, J. S. Wolenski, E. M. Espreafico, P. Forscher, R. E. Larson, and M. S. Mooseker. 1993. Brain myosin-V is a two-headed unconventional myosin with motor activity. *J. Cell Biol.* 75:13–23.

Davis, N. G., J. L. Horecka, and G. F. Sprague. 1993. *Cis-* and *trans*-acting functions required for endocytosis of the yeast pheromone receptors. *J. Cell Biol.* 122:53–65.

Esmon, B., P. Novick, and R. Schekman. 1981. Compartmentalized assembly of oligosaccharides on exported glycoproteins in yeast. *Cell.* 25:451–460.

Espindola, F. S., E. M. Espreafico, M. V. Coelho, A. R. Martins, F. R. C. Costa, M. S. Mooseker, and R. E. Larson. 1992. Biochemical and immunological characterization of p190-calmodulin complex from vertebrate brain: a novel calmodulin-binding myosin. *J. Cell Biol.* 118:359–368.

Espreafico, E. M., R. E. Cheney, M. Matteoli, A. A. C. Nascimento, P. V. De Camilli, R. E. Larson, and M. S. Mooseker. 1992. Primary structure and cellular localization of chicken brain myosin-V (p190), an unconventional myosin with calmodulin light chains. *J. Cell Biol.* 119:1541–1557.

Fath, K. R., G. M. Trimbur, and D. R. Burgess. 1994. Molecular motors are differentially distributed on Golgi membranes from polarized epithelial cells. *J. Cell Biol.* 126:661–675.

Franzusoff, A., and R. Schekman. 1989. Functional compartments of the yeast Golgi apparatus are defined by the *sec7* mutation. *EMBO (Eur. Mol. Biol. Organ.) J.* 8:2695–2702.

Franzusoff, A., K. Redding, J. Crosby, R. S. Fuller, and R. Schekman. 1991. Localization of components involved in protein transport and processing through the Golgi apparatus. *J. Cell Biol.* 112:27–37.

Graham, T. R., and S. D. Emr. 1991. Compartmental organization of Golgi-specific protein modification and vacuolar protein sorting events defined in a yeast *sec18* (NSF) mutant. *J. Cell Biol.* 114:207–218.

Haarer, B. K., S. H. Lillie, and S. S. Brown. 1994. Identification of *MYO4*, a second class V myosin gene in yeast. *J. Cell Sci.* 107:1055–1064.

Hall, D. H., and E. M. Hedgecock. 1991. Kinesin-related gene *unc-104* is re-

quired for axonal transport of synaptic vesicles in *C. elegans*. *Cell.* 65: 837–847.

Holtzman, D. A., S. Yang, and D. G. Drubin. 1993. Synthetic-lethal interactions identify two novel genes, *SLA1* and *SLA2*, that control membrane cytoskeleton assembly in *Saccharomyces cerevisiae*. *J. Cell Biol.* 122: 635–644.

Huffaker, T. C., J. H. Thomas, and D. Botstein. 1988. Diverse effects of β-tubulin mutations on microtubule formation and function. *J. Cell Biol.* 106:1997–2010.

Ito, H., Y. Fukuda, K. Murata, and A. Kimura.1983. Transformation of intact yeast cells with alkali cations. *J. Bacteriol.* 153:163–168.

Johnston, G. C., J. A. Prendergast, and R. A. Singer. 1991. The *Saccharomyces cerevisiae MYO2* gene encodes an essential myosin for vectorial transport of vesicles. *J. Cell Biol.* 113:539–551.

Julius, D., R. Schekman, and J. Thorner. 1984*a*. Glycosylation and processing of prepro-α-factor through the yeast secretory pathway. *Cell.* 36:309–318.

Julius, D., A. Brake, L. Blair, R. Kunisawa, and J. Thorner. 1984*b*. Isolation of the putative structural gene for the lysine-arginine-cleaving endopeptidase required for processing of yeast prepro-α-factor. *Cell.* 37:1075–1089.

Kaiser, C. A., and R. Schekman. 1990. Distinct sets of *SEC* genes govern transport vesicle formation and fusion early in the secretory pathway. *Cell.* 61:723–733.

Kaneko, Y., N. Hayashi, A. Toh-e, I. Banno, and Y. Oshima. 1987. Structural characteristics of the *PHO8* gene encoding repressible alkaline phosphatase in *S. cerevisiae*. *Gene (Amst.).* 58:137–148.

Kilmartin, J. V., and A. E. M. Adams. 1984. Structural rearrangements of tubulin and actin during the cell cycle of the yeast *Saccharomyces*. *J. Cell Biol.* 98:922–933.

Klionsky, D. J., and S. D. Emr. 1989. Membrane protein sorting: biosynthesis, transport and processing of yeast vacuolar alkaline phosphatase. *EMBO (Eur. Mol. Biol. Organ.) J.* 8:2241–2250.

Kubler, E., and H. Riezman. 1993. Actin and fimbrin are required for the internalization step of endocytosis in yeast. *EMBO (Eur. Mol. Biol. Organ.) J.* 12:2855–2862.

Kubler, E., F. Schimmoller, and H. Riezman. 1994. Calcium-independent calmodulin requirement for endocytosis in yeast. *EMBO (Eur. Mol. Biol. Organ.) J.* 13:5539–5546.

Kuznetsov, S. A., G. M. Langford, and D. M. Weiss. 1992. Actin-dependent organelle movement in squid axoplasm. *Nature (Lond.).* 356:722–725.

Lillie, S. H., and S. S. Brown. 1992. Suppression of a myosin defect by a kinesin-related gene. *Nature (Lond.).* 356:358–361.

Lillie, S. H., and S. S. Brown. 1994. Immunofluorescence localization of the unconventional myosin, Myo2p, and the putative kinesin-related protein, Smy1p, to regions of growth in *Saccharomyces cerevisiae*. *J. Cell Biol.* 125:825–842.

Liu, H., and A. Bretscher. 1992. Characterization of *TPM1* disrupted yeast cells indicates an involvement of tropomyosin in directed vesicular transport. *J. Cell Biol.* 118:285–299.

Madden, K., C. Costigan, and M. Snyder. 1992. Cell polarity and morphogenesis in *Saccharomyces cerevisiae*. *Trends Cell Biol.* 2:22–29.

Mercer, J. A., P. K. Seperack, M. C. Strobel, N. G. Copeland, and N. A. Jenkins. 1991. Novel myosin heavy chain encoded by Murine *dilute* coat color locus. *Nature (Lond.).* 349:709–712.

Mulholland, J., D. Preuss, A. Moon, A. Wong, D. Drubin, and D. Botstein. 1994. Ultrastructure of the yeast actin cytoskeleton and its association with the plasma membrane. *J. Cell Biol.* 125:381–391.

Novick, P., and R. Schekman. 1983. Export of major cell surface proteins is blocked in yeast secretory mutants. *J. Cell Biol.* 96:541–547.

Novick, P., and D. Botstein. 1985. Phenotypic analysis of temperature-sensitive yeast actin mutants. *Cell.* 40:405–416.

Novick, P., C. Field, and R. Schekman. 1980. Identification of 23 complementation groups required for post-translational events in the yeast secretory pathway. *Cell.* 21:205–215.

Novick, P., S. Ferro, and R. Schekman. 1981. Order of events in the yeast secretory pathway. *Cell.* 25:461–469.

Preuss, D., J. Mulholland, A. Franzusoff, N. Segev, and D. Botstein. 1992. Characterization of the *Saccharomyces* Golgi complex through the cell cycle by immunoelectron microscopy. *Mol. Biol. Cell.* 3:789–803.

Raths, S., J. Rohrer, F. Crausaz, and H. Riezman. 1993. *end3* and *end4*: two mutants defective in receptor-mediated and fluid-phase endocytosis in *Saccharomyces cerevisiae*. *J. Cell Biol.* 120:55–65.

Raymond, C. K., I. Howald-Stevenson, C. A. Vater, and T. H. Stevens. 1992. Morphological classification of the yeast vacuolar protein sorting mutants: evidence for a prevacuolar compartment in class E *vps* mutants. *Mol. Biol. Cell.* 3:1389–1402.

Rexach, M. F., and R. Schekman. 1991. Distinct biochemical requirements for the budding, targeting and fusion of ER-derived transport vesicles. *J. Cell Biol.* 114:219–229.

Salama, N. R., T. Yeung, and R.W. Schekman. 1993. The Sec13p complex and reconstitution of vesicle budding from the ER with purified cytosolic proteins. *EMBO (Eur. Mol. Biol. Organ.) J.* 12:4073–4082.

Salminen, A., and P. J. Novick. 1987. A *ras*-like protein is required for a post-Golgi event in yeast secretion. *Cell.* 49:527–538.

Sherman, F., G. Fink, and C. Lawrence. 1974. Methods in Yeast Genetics. Cold Spring Harbor Laboratory, Cold Spring Harbor, New York.

Stevens, T., B. Esmon, and R. Schekman. 1982. Early stages in the yeast secretory pathway are required for transport of carboxypeptidase Y to the vacuole. *Cell.* 30:439–448.

Titus, M. A. 1993. From fat yeast and nervous mice to brain myosin-V. *Cell.* 75:9–11.

Vida, T. A., G. Huyer, and S. D. Emr. 1993. Yeast vacuolar proenzymes are sorted in the late Golgi complex and transported to the vacuole via a prevacuolar endosome-like compartment. *J. Cell Biol.* 121:1245–1256.

Walworth, N., and P. Novick. 1987. Purification and characterization of constitutive secretory vesicles from yeast. *J. Cell Biol.* 105:163–174.

Watts, F. Z., G. Shiels, and E. Orr. 1987. The yeast *MYO1* gene encoding a myosin-like protein required for cell division. *EMBO (Eur. Mol. Biol. Organ.) J.* 6:3499–3505.

Welch, M. D., D. A. Holtzman, and D. G. Drubin. 1994. The yeast actin cytoskeleton. *Curr. Opin. Cell Biol.* 6:110–119.

Wilcox, C., and R. S. Fuller. 1991. Posttranslational processing of the prohormone-cleaving Kex2 protease in the *Saccharomyces cerevisiae* secretory pathway. *J. Cell Biol.* 115:297–307.